Advances in Science and Technology Research Journal

Advances in Science and Technology Research Journal, 2025, 19(3), 341–349
https://doi.org/10.12913/22998624/197407
ISSN 2299-8624, License CC-BY 4.0

Received: 2024.11.08
Accepted: 2025.01.15
Published: 2025.02.01

Vibrations and impact forces of modified handle pneumatic hammer

Tadeusz Majewski[1,2*], Marco Meraz Melo[1], Jan Tracz[2], Edyta Ładyżyńska-Kozdraś[2], Quirino Estrada[3]

[1] Tecnologico Nacional De Mexico, Instituto Tecnologico de Puebla, Av. Tecnologico 420, Col. Maravillas Puebla, Pue. C.P. 72220, Mexico
[2] Warsaw University of Technology, Wydzial Mechatroniki, Warszawa, ul. Swietego Boboli 8, 02-525 Warszawa, Poland
[3] Universidad Autónoma de Ciudad Juarez, Campus Ciudad Cuauhtemoc, Chihuahua, Mexico
* Corresponding author's e-mail: t24majewski@gmail.com

ABSTRACT

The paper presents a dynamic model of a small electro-pneumatic percussive tool whose handle is elastically connected to the casing. The pneumatic force is defined as a function of the position of the piston and the striker. The Hertz model has been applied to the impact forces and given the conditions under which they exist. The differential equations define the movement of each part of the hammer. Their simulations show how the hammer parts vibrate, when the impacts occur, and how large the impact forces can be. The acceleration of the handle is determined and compared with the acceleration when the handle is part of the casing. The article proves that the hammer with a floating handle is better for the operator's protection.

Keywords: vibrations, impact hammer, impact forces, handle vibrations, efficiency.

INTRODUCTION

Vibration and impact are essential features of many domestic and industrial hand-held machines. They all produce vibrations and noise that are harmful to people. They cause stress, irritation, and reduced mental performance, and long-term use of hammers can cause illness. Hammers come in different sizes, shapes, and operating principles. The small ones may have a mechanical working principle, the more sophisticated ones have an internal pneumatic chamber, and the most powerful hammers use external compressed air. Pneumatic impact tools have many industrial and commercial applications.

Vibration experts and designers of hand-held tools are looking for ways to eliminate or reduce their vibration. Special gloves can reduce the vibrations transmitted to the operator's hand [1]. Permissible exposure to vibration depends on the vibration level and time [2]. Leading manufacturers of hand tools, such as Makita, Bosch, and DeWalt, apply their methods to absorb, reduce, or dissipate the vibrations produced by power tools. One of them is an additional mass that moves in an opposite direction to the piston, the other uses impact masses whose motion is controlled by the pressure of both sides of the piston [3].

Existing articles attempt to describe the dynamic process of percussion tools using some simplifications or assumptions that may not always be valid for impact motion [4–9].

The dynamics of percussion machines are complicated by the multiple impacts that make the problem complex and difficult to analyze. The article tries to define the sequence of the impacts and the forces they cause. It was shown that a pneumatic hammer with a floating handle better protects the operator, and the modification does not decrease the efficiency of the hammer.

PRINCIPLE OF A PNEUMATIC HAMMER

A viscous-elastic component connects the handle to the hammer body, typically stabilized by four initial compression springs. The hammer comprises five main parts: handle 1, hammer body 2, slider-crank mechanism OAB, striker 3, and chisel 4. The pushing force P is transmitted to the chisel via the buffer E. Power from the electric motor is transferred to the crank through a gear system, inducing a reciprocating motion of the piston. The crank's speed ω is four times faster than the motor's. As the distance between the piston and the striker varies, so does the pressure, resulting in a pneumatic force F_p that pushes the striker against the chisel. Their collision produces an impact force F_3, causing the chisel to impact the object with force F_4, resulting in the removal of material from object 5, followed by another impact of the chisel with force F_5 against the casing (Fig. 1).

DYNAMIC MODEL OF THE HAMMER

How the hammer behaves depends on the external and internal forces acting on it. These should be accurately defined to know the behavior of the hammer, its useful properties, and the vibrations transmitted to the operator. The mass of the hammer body is M and the handle with part of the operator's arm has the mass m_1. The viscoelastic properties of the operator's shoulder are k_1 and c_1, the connection of the handle to the casing is k_2 and c_2, and the buffer is k_5 and c_5. The position of the handle is defined by the coordinate x_1, the position of the hammer body by x, and the position of the striker and chisel relative to the hammer by z_3 and z_4. The operator pushes the handle with a force P, which gives the displacement of the operator's hand x_0, and the reciprocating movement of the piston gives rise to a pneumatic force F_p and an inertial force B_p. When two adjacent parts come into contact, the impact forces are generated: between the striker 3 and the chisel 4, then the chisel and the face F. The crank OA rotates at an angular velocity ω and the angle $\alpha = \omega t$ defines its position – Fig. 2. The relation between the angles α and β

$$\sin(\beta) = \frac{r}{l}\sin(\alpha) \tag{1}$$

The relative position of the piston z_p to the hammer casing

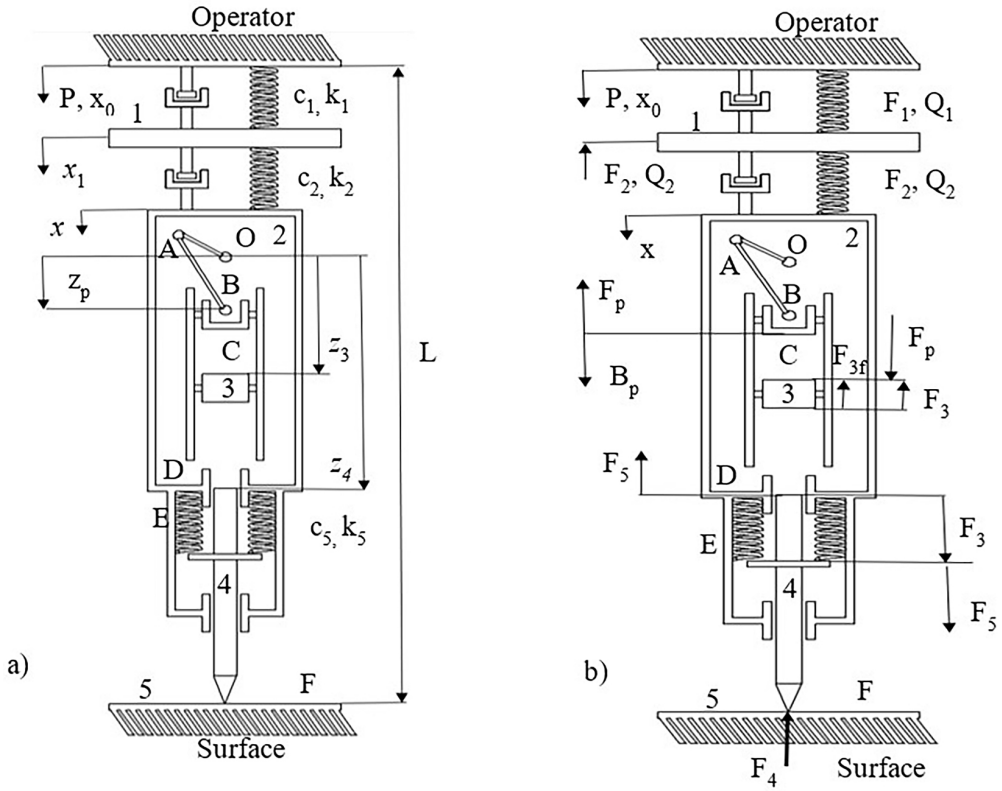

Figure 1. Sketch of the hammer (a) and the forces occurring in the system (b), 1 – handle, 2 – casing, 3 – striker, 4 – chisel, 5 – demolished object or treated surface

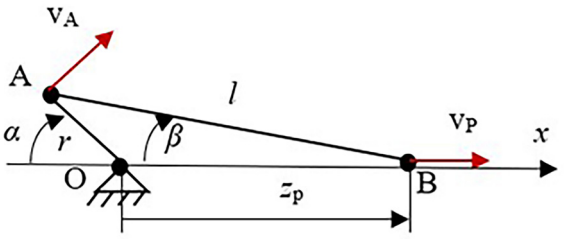

Figure 2. Crank mechanism; OA – crank, AB – connecting rod, B – piston

$$z_p = l\sqrt{1-(\frac{r}{l}sin\alpha)^2} - rcos\alpha \quad (2)$$

The velocity of the piston changes as below

$$v_p = r\omega\frac{\sin(\alpha-\beta)}{\cos(\beta)} \quad (3)$$

The variety velocity of the piston gives the inertial force B_p.

$$B_p = -m_p a_p = -m_p\frac{dv_p}{dt} \quad (4)$$

The change of the distance between the piston and the striker in chamber C results in compression or expansion of the air and the pneumatic force F_p acting on the piston and striker. The distance between them d_{23} is defined as follows.

$$d_{23} = (z_{30} + z_3) - z_p \quad (5)$$

where: z_{03} is the initial position of the striker relative to the origin of the crank O and z_3 is the instantaneous striker position. The temperature of the air in the chamber stabilizes during the hammer work and Boyle's - Mariotte's Law can be applied.

$$pV = p_0V_0 \quad (6)$$

where: p_0 is the atmospheric pressure, V_0 is the initial volume of the air in the chamber, and p and V are the instantaneous pressure and volume of the chamber.

$$V_0 = A \times (z_{30} - (l-r))$$
$$V = A \times (z_{30} + z_3 - z_p) \quad (7)$$

where: d is the diameter of the striker and A = $\pi d^2/4$ its area.

The pressure of the air at any instant

$$p = p_0\frac{z_{30}-(l-r)}{z_{30}+z_3-z_p} \quad (8)$$

One side of the striker has the pressure p and the other p_0. The pneumatic force F_p acting on the striker is the result of the difference between them.

$$F_p = A\Delta p = A(p-p_0) = A\frac{V_0-V}{V}p_0 = A\frac{\Delta V}{V}p_0 \quad (9)$$

where:

$$\Delta V = A[z_p - z_3 - (l-r)] \quad (10)$$

The pneumatic force is a non-linear function of the piston and striker position z_3

$$F_2 = \frac{z_p-z_3-(l-r)}{z_{30}+z_3-z_p}F_{20} \quad (11)$$

where: $F_{20} = Ap_0$.

The motion of the hammer components depends on the forces acting on each of them, as depicted in Fig. 1b, and is governed by the following set of differential equations:

The handle of the hammer

$$1.\, m_1\ddot{x}_1 = G_1 + P - (F_1 + Q_1) - (F_2 + Q_2) \quad (12)$$

where: $P = k_1x_0$, the forces F_1, Q_1 present the viscoelastic properties of the operator's arm and F_2, Q_2 the viscoelastic properties of the connection of the handle to the hammer, $G_1 = m_1g$ is the component of gravity on direction of the hammer axis, $g = g_0\cos\gamma$, $g_0 = 9.8$ m/s^2, $\gamma \in (0, \pi)$ is the angle of the hammer position concerning the vertical direction.

The motion of the hammer's casing (the heaviest part) is governed by the following equation

$$2.\, M\ddot{x} = G + (F_2 + Q_2) - F_p + B_p - (F_5 + Q_5) - Q_{2M} \quad (13)$$

where: F_p is the pneumatic force acting on the piston, B_p is the inertia force from the motion of the piston with respect to the cassing, F_5 and Q_5 are the forces from the buffer E, Q_{2M} is the viscous force, $G = Mg$ is the component of the hammer gravity.

The relative position of the striker to the hammer´s casing

$$3.\, m_3\ddot{z}_3 = G_3 - m_3\ddot{x} + F_p - F_f - (F_3 + F_{3r}) \quad (14)$$

where: F_f -is the friction force of the striker, F_3, F_{3r} are the impact and damping forces when the striker and chisel are in contact.

The relative position of the chisel concerning the hammer´s casing

$$4.\, m_4\ddot{z}_4 = G_4 - m_4\ddot{x} + (F_3 + F_{3r}) - (F_4 + F_{4r}) + (F_5 + Q_5) \quad (15)$$

where: F_4, F_{4r} are the forces when the chisel impacts against the surface F (elastic and damping).

The stiffness coefficients k_i and damping coefficients c_i define the characteristics of springs 1, 2, and 5. The impact forces exist only when the parts are in contact. The Hertzian model of elastic bodies was used to determine the impact forces: between the steel striker and the steel chisel as two cylinders in contact with their flat surfaces and the contact of the chisel with the surface F as a cylinder (radius r = 2 mm, length L = 20 mm) with the elastic half-space of mineral asphalt mixture or concrete [10, 11 pegs. 55–60]. For the numerical study, they were taken as; k_3 the stiffness of the striker/chisel contact with magnitude from 10^7 to 10^8 N/m, and the contact chisel/treated surface k_4 from 5×10^6 to 5×10^7 N/m. Impact force limitations:

$$\text{If } d_{23} = \Delta_3 = z_2 + z_{20} - (z_3 + z_{30}) \geq 0 \text{ then}$$
$$F_3 = k_3 \Delta_3 \text{ else } F_3 = 0 \quad (16)$$

$$\text{If } d_4 = \Delta_4 = x + z_3 + z_{30} \geq 0 \text{ then}$$
$$F_4 = k_4 \Delta_4 \text{ else } F_4 = 0 \quad (17)$$

A part of the energy is dissipated during impacts. Usually, it is defined by the coefficient of restitution χ; which can be known from the experiment.

$$\chi = v_r/v \quad (18)$$

where: v is the velocity before the impact and v_r is the rebound velocity. A loss of energy ΔT during the impact can be written as

$$\frac{\Delta T}{T} = \frac{T - T_r}{T} = \frac{0.5mv^2(1-\chi^2)}{0.5mv^2} = (1-\chi^2) \quad (19)$$

The energy loss will be simulated by a friction force F_r that is proportional to the impact force F_i as shown in Fig. 3. The resistance forces F_r were taken as proportional to the impact forces.

$$F_{3r} \cong p_3 F_3 sign(v_{34}) \quad (20)$$

$$F_{4r} \cong p_4 F_4 sign(v_{40}) \quad (21)$$

where: the coefficients p_3 and p_4 present the percentages of dissipated energy, v_{34}, v_{40} are the velocities of the penetration.

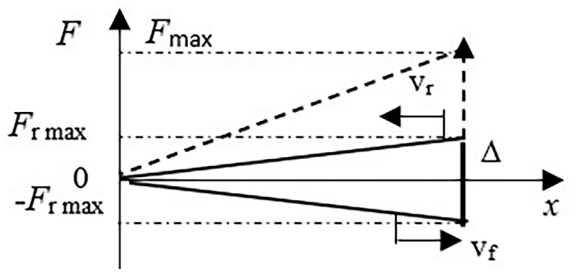

Figure 3. Change of the friction force F_r with the indentation Δ

Energy loss during impact

$$W_r = \int F_r d\Delta \approx F_{rmax}\Delta \quad (22)$$

can be approximated by a triangle as shown in Fig. 3 where F, F_r are the impact and the friction forces, Δ is the depth of penetration. The coefficient p_4 the chisel´s impact represents the energy dissipated by friction and the energy used to remove some material from the surface.

The dissipated energy W_r from the resistance force F_r during indentation (Fig. 3) is $W_r \cong pF_{max}\Delta$ while the elastic energy of the indentation is $V = 0.5\Delta F_{max}$. The coefficient of restitution was taken as 0.95 – 98 for the striker/chisel impact and 0.9 - 0.95 for the chisel/surface impact.

The efficiency of the hammer depends on the chisel energy when it impacts against the surface.

$$\text{if } x + z_4 > 0$$
$$T_h = \frac{1}{2} m_4 (\dot{x} + \dot{z}_4)^2 \quad (23)$$

A part of this energy is used to remove a little bit of material from the surface for each impact.

SIMULATION OF HAMMER BEHAVIOR

Dealing with multiple impacts, non-linearity, and non-continuous differential equations poses a complex challenge, necessitating numerical methods to assess the behavior of the hammer and its potential outcomes. The parameters of the MAKITA hammer model DWD024-B3 VVR, equipped with a rigid handle, were used to analyze the properties of the hammer with a floating handle.

The vibrations of the un-modified hammer were measured using a B&K 4507B accelerometer and the sensitivity of the measuring system is 0.24 ms²/mV, the acceleration and its spectrum are shown in Fig.4. The operator´s pushing force was not measured. The acceleration of the hammer after the chisel rebound from the surface F is between -190 and -250 m/s² with a frequency of 57.3 Hz. The vibrations between the successive chisel impacts are smaller because of the hammer's internal parts impacts. The amplitudes of the first three harmonics of acceleration are 22, 20.3, and 28.6 ms^{-2}.

The parameters of the hammer with floating handle: $m_1 = 0.5$ kg, $M = 4.5$ kg, $m_3 = 0.075$ kg, $m_4 = 0.25$ kg. Other parameters: $k_1 = k_2 = 2$ kN/m, k_5 from 20 to 40 kN/m, pushing force P is from 0 to 300 N, the hammer can be situated in any direction so there is also the gravity force G. The influence

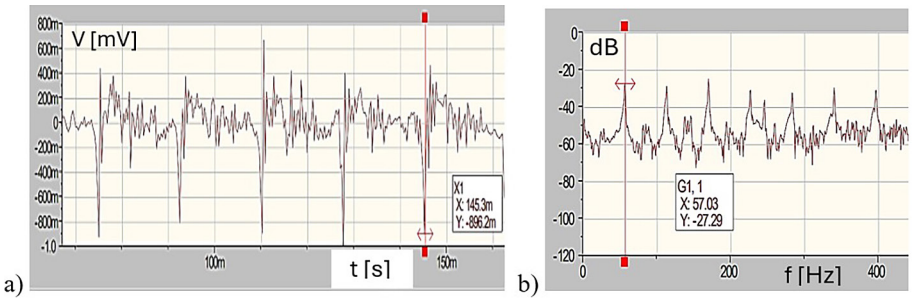

Figure 4. Acceleration (a) of the unmodified hammer and its frequency spectrum (b)

of the stiffness k_3, k_4 were taken from 5×10^6 to 10^8 N/m, and 10^6 to 5×10^7 N/m, respectively.

The diagrams presented below show the behavior of the system and the change of the most important parameters of the hammer with the crank rotation $\tau = \alpha = \omega t$ [rad]; the positions, the accelerations, and the impact forces when the initial displacement of the operator´s palm is $x_0 = 25$ mm (pushing force $P = 50$ N), $k_3 = 5 \times 10^7$ N/m, $k_4 = 10^7$ N/m, $k_4 = 2 \times 10^7$ N/m. The operator's body is fixed, and the palm is displaced x_0 to generate the pushing force P_0. As observed, the vibrations of both the casing and handle exhibit irregular patterns. The casing´s position fluctuates between -25 mm and 2 mm, while the handle´s position varies between -12 mm and 4 mm. Notably, the handle´s vibrations mirror those of the casing but on a smaller scale. The hammer´s casing retracts approximately 10 mm, whereas the handle retracts about 5 mm.

The casing vibrates with the acceleration from the range -250 m/s^2 to 70 m/s^2 (sometimes -400 m/s^2) while the handle from -35 m/s^2 to 50 m/s^2 (sometimes -140 m/s^2). The harmful acceleration a_{x1} acting on the operator is almost five times lower than the case acceleration Fig 6b. When the handle is rigidly connected to the hammer, its maximum acceleration is almost three times higher than that of the floating handle Fig 5c (170m/s^2 vs. 50 m/s^2). It can also be seen that the acceleration of the casing of the hammer with the floating handle is greater than that of the unmodified hammer. The positive acceleration of the hammer body varies slightly depending on the system parameters, but it's been shown that the negative acceleration of the chisel rebound is several times greater and more complex than positive acceleration. Smaller vibrations of the floating handle protect the operator better and higher vibrations of the casing can improve the useful parameters of the hammer, i.e., the impact force of the chisel and its impact energy. The impact forces F_4 and F_3 are shown in Fig.

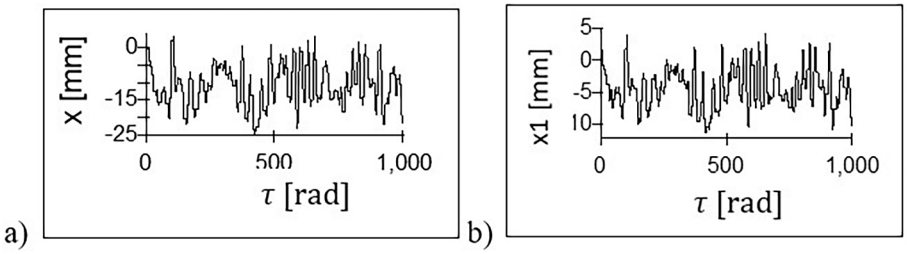

Figure 5. Position of the hammer casing (a) and the handle (b)

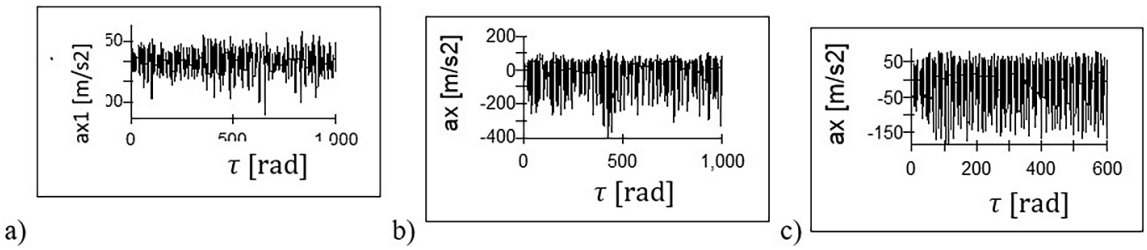

Figure 6. Accelerations of the handle (a), the casing (b), and the casing of the unmodified hammer (c)

6. The impact force of the chisel F_4 can reach up to 9 kN while the impact force of the striker can reach up to 20 kN. The frequency of the chisel´s vibration is approximately twelve times higher than that of the striker´s vibrations. This higher frequency is due to three impacts: from the striker, the buffer, and the surface F. The impact force F_4 occurs when the chisel touches the surface $df_4 = x + z_4 > 0$ – Fig. 7a.

It can be observed that the chisel can be drawn back from the surface up to 30 mm (Fig. 8a), the penetration of the chisel can be up to 0.8 mm (Fig. 8b), one of them enters the surface 0.4 mm and the time of contact is 0.5 ms (Fig. 8c). Suppose the stiffness between the impacting elements is five times lower, e.g., k_3 =10^7 N/m, k_4=5 × 10^6 N/m, and the pressing force is P = 50 N then after about 2 seconds the vibrations of the casing, handle, and chisel will decrease to a very low level and the impact force disappears, as shown in Figure 9.

In this case, the hammer does not execute its function, and the operator must increase the pushing force P. Increasing the force up to P = 100 N stabilizes the hammer's work as shown in Fig. 10.

The hammer behavior was studied for three sets of the impact stiffnesses to verify their influence on the hammer work; k_3 = 10^7, 5 × 10^7, 10^8 N/m and k_4 = 5 × 10^6, 10^7, 5 × 10^7 N/m, respectively. It was observed that the vibrations and accelerations of the casing and the handle change a little, a little more the energy of the chisel impact,

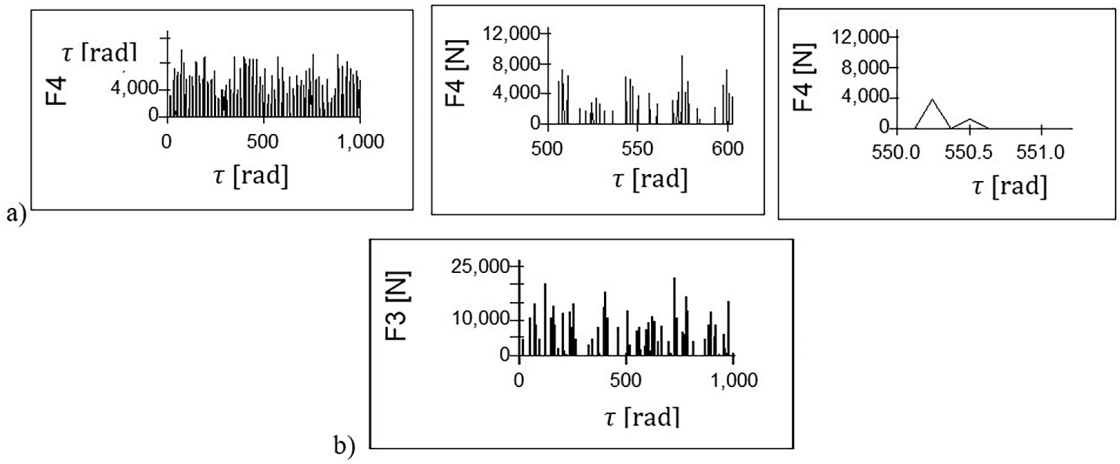

Figure 7. Impact force F_4 of the chisel for different time spans (a) and the striker F_3 (b)

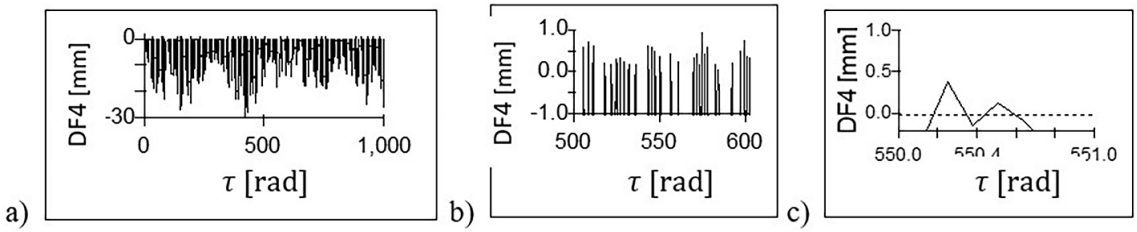

Figure 8. Position of the chisel concerning the surface DF4 = $x + z_4$ (a) and the chisel´s penetration Δ (b, c)

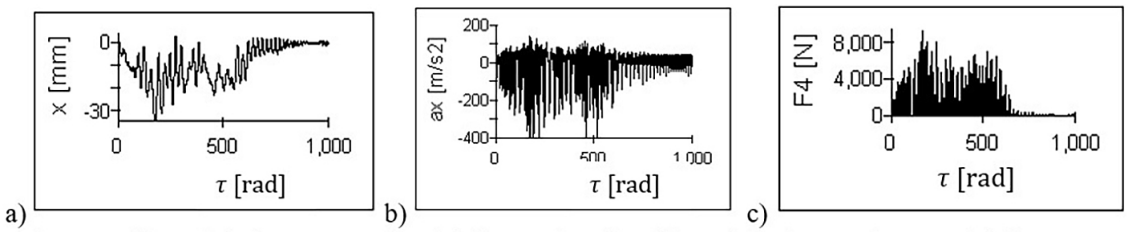

Figure 9. Position of the hammer casing (a), its acceleration (b), and the impact force F_4 (c) for P = 50 N

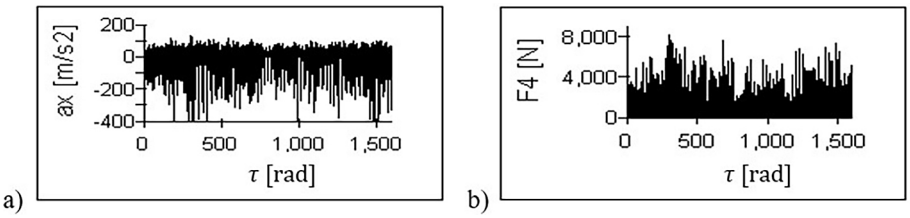

Figure 10. Acceleration of the casing (a) and the impact force F_4 (b) for $P = 100$ N

but with the increase of the stiffnesses k_3, k_4 the forces F_3 and F_4 increase significantly, as shown in Figure 11.

The efficiency of the hammer depends on the chisel´s energy when it impacts the surface.

If $x + z_4 > 0$

$$T_h = \frac{1}{2} m_4 (\dot{x} + \dot{z}_4)^2 \qquad (22)$$

A part of this energy is used to remove some material from the surface F. The diagram Fig. 12 shows the change of the impact energy in time, more impacts have the power of about 2 J and its maximum magnitude can be up to 7 J.

If the stiffnesses are $k_3 = 5 \times 10^7$, $k_4 = 10^7$ N/m, and the pressing force P increases from 0 to 200 N, maximum force F_3 increases by about 70% and the impact force F_4 increases by about 50%, the other parameters such as the accelerations of the handle and the casing, the impact energy T change slightly.

On the other hand, if the pressing force $P = 100$ N remains constant, but the stiffness between the elements increases tenfold, from $k_3 = 10^7$, $k_4 = 5 \times 10^6$ N/m to $k_3 = 10^8$, $k_4 = 5 \times 10^7$ N/m, then the maximum force F_3 increases by about three times and F_4 two and a half times – Fig. 13a. The other

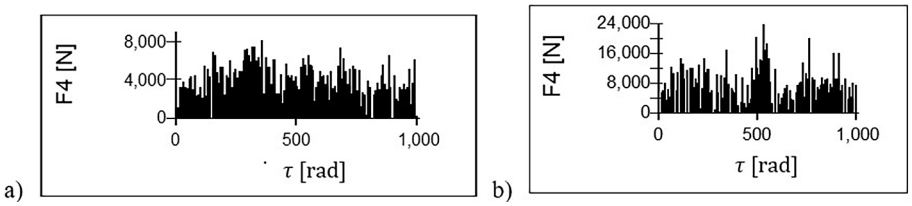

Figure 11. Impact force F_4 for $k_3 = 10^7$ N/m, $k_4 = 5 \times 10^6$ N/m (a) and $k_3 = 10^8$ N/m, $k_4 = 5 \times 10^7$ N/m (b)

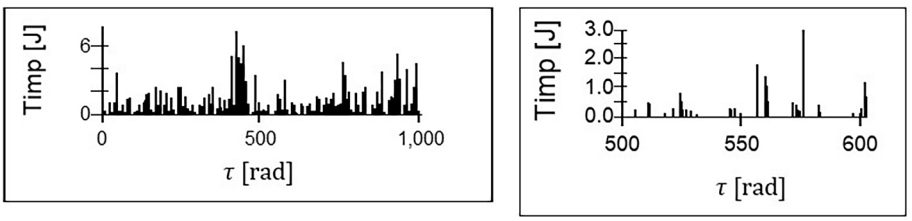

Figure 12. Energy of the chisel when it impacts the surface

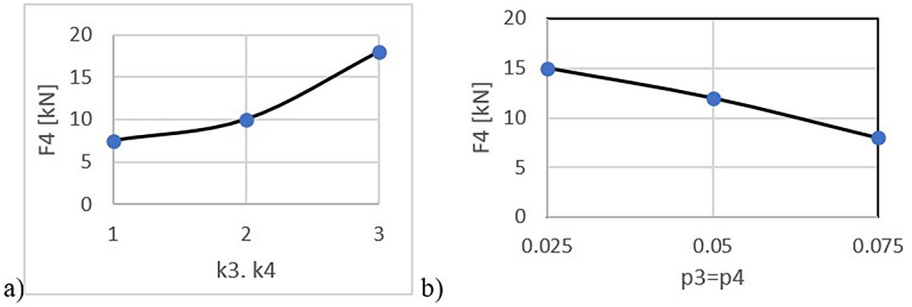

Figure 13. Impact force F_4 if $P = 100$ N for: 1. $k_3 = 10^7$ N/m, $k_4 = 5 \times 10^6$ N/m; 2. $k_3 = 5 \times 10^7$ N/m, $k_4 = 10^7$ N/m; 3. $k_3 = 10^7$ N/m, $k_4 = 5 \times 10^7$ N/m as a function of the resistance $p_3 = p_4$

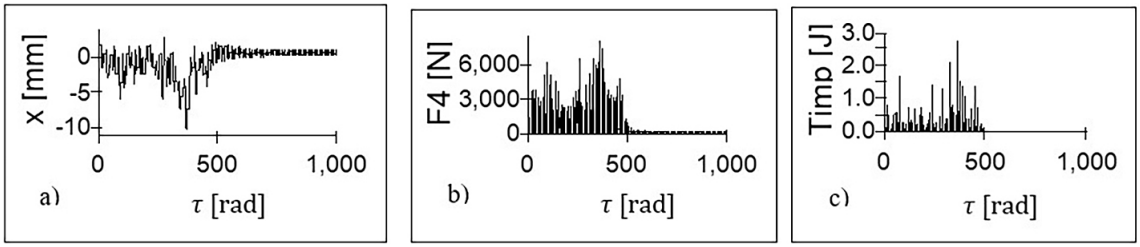

Figure 14. Position of the hammer casing (a), the impact force F_4 (b), and the impact energy, (c) if $P = 300$ N, $p_3 = 0.05$, $p_4 = 0.1$

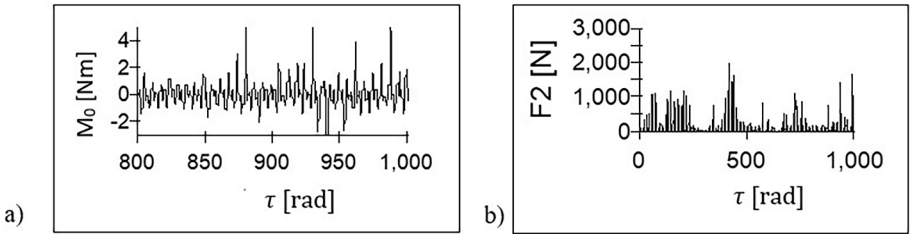

Figure 15. Change of the torque M_0 (a) and the pneumatic force F_2 (b) with the crank rotation

parameters defining the behavior of the hammer change only marginally.

If the impact damping p_3, p_4 rise, then the impact forces fall – Fig. 13b. At a certain level of damping, the chisel and the casing vibrations disappear, e.g., for the pressing force of 100 N (x_0 = 25 mm) and $p_3 = p_4 = 0.1$ the vibrations stop, and the tool no longer functions as a hammer.

Another conclusion that can be drawn from the numerical simulation is the influence of the energy dissipated during the impacts. The striker and chisel are made of steel and their coefficient of restitution is constant, while the chisel can impact different surfaces, resulting in an increase or decrease of the dissipated energy. If the impacts of the striker/chisel dissipate 10% ($p_3 = 0.05$) of the energy, then the impact of the chisel on the surface can dissipate up to 20% ($p_3 = 0.1$) of the chisel energy if the pushing force $P \geq 100$ N – Fig. 13b.

Once the damping effect is too high ($p_3 = p_4 > 0.075$), the vibrations of the chisel decrease, and the tool loses its hammer function. The same applies to increasing the operator pressing force to 300 N, the tool loses its dynamic properties as a hammer, and the vibrations and the impact force decrease over time, as shown in Figure 14.

To keep the rotation of the crank and reciprocating motion of the piston there should be a propulsion torque M_0 that overcomes the pneumatic force F_p and the inertia force of the piston $m_p(\ddot{x} + a_p)$. The dynamic equilibrium of the crank mechanism (Fig. 2) is as follows.

$$M_O = r\frac{\cos(\alpha-\beta)}{\cos(\beta)}[F_p - m_p(\ddot{x} + a_p)] \quad (23)$$

The diagram Figure 15 shows the variation of the torque M_0 with the position of the crank. The inertia force of the piston B_p can be up to 180 N, and the pneumatic force F_p can reach up to 300 N, but the buffer force F_5 can be several times higher than F_p. The variation of the torque M_0 can change the angular velocity of the crank (analysis not shown here) and the hits between the teeth in the gear system would generate noise. If the angular velocity of the crank is i_v times higher than the motor, then the motor should give a torque. $M_E > i_v M_O$ and the required power of the electric motor

$$P_E \cong i_v M_0 \omega_E \quad (24)$$

If the torques M_E and M_0 are known, then the magnitude of the hammer torque limiter can be adjusted. When the average moment is about 1.5 Nm then the motor should have the power of 540 W for the hammer function of the tool while the power of the motor of Makita HR2511 is 800 W.

The results of the simulation are given for constant initial shoulder displacement x_0.

CONCLUSIONS

The article demonstrated the movement of the hammer parts, the magnitude of the impact forces, and the energy that the chisel can transfer to the treated surface. The pneumatic chamber between the piston and the striker separates the mechanical impacts between the parts from the casing.

The frequency of the chisel substantially exceeds that of the striker. The elastic connection of the handle to the casing significantly reduces the vibrations transmitted to the operator. This modification better protects the tool's users and does not reduce its efficiency. The impact forces are characterized by a very short time of action (milliseconds) and high magnitude (several kN), while the energy of the chisel impact can reach up to 6 J. It has been shown that the hammering function of the percussion tool can be maintained if the energy loss during penetration is less than 20% of the chisel. The operator must work with the hammer to exploit its abilities by increasing or decreasing the pushing force. During the work, the impact forces pull the hammer back from the demolishing object or treated surface. The dynamic model can be used to find the optimal parameters of the hammer, its higher efficiency, and at the same time better protection for the user. The versatility of this model goes beyond a specific hammer and can be applied to various percussion tools.

REFERENCES

1. Herman T., Dobry M.W. Energy evaluation of protection effectiveness of anti-vibration gloves, International Journal of Occupational Safety and Ergonomics, 2017, 23(3), 414–423, https://doi.org/10.1080/10803548.2016.1233673
2. PN-EN ISO 5349-2:2004
3. https://www.ereplacementparts.com/makita-hr2511-rotary-hammer-parts-c-97_380_490.html
4. Khulief Y.A., Shabana A.A. A continuous force model for the impact analysis of flexible multibody systems, Mechanism and Machine Theory, 1987, 22(3), 213–224, https://doi.org/10.1016/0094- 114x(87)90004-8
5. Babitsky V.I. Hand-held percussion machine as discrete non-linear converter, Journal of Sound and Vibration, 1998, 214(1), 165–182. https://doi.org/10.1006/jsvi.1998.1559
6. Li F., Ma S. Analysis and experimental study of acceleration model for short interval and multiple impact equipment, Shock and Vibration, 2019, ID5139137 https://doi.org/10.1155/2019/5139137
7. Rajalingham C., Rakheja S. Analysis of impact force variation during the collision of two bodies using a single-degree-of-freedom system model, Journal of Sound and Vibration, 2000, 229(4), 27, 823–835.
8. Pfeiffer F., Locker Ch. Contacts in multibody systems, Journal of Applied Mathematics and Mechanics, 2000, 64(5), 773–782, https://doi.org/10.1016/S0021-8928(00)00107-6
9. Auguściński A., Talaśka K., Wilczyński D. External dynamics of hand operated hydraulic hammer, Machine Dynamics Problems, 2008, 32(1), 7–13.
10. Zimmerman J., Majewski T., Rymuza Z. Modeling of the nanoindentation process of ultrathin films. International Journal of Material Research Zeitschrift fur Metallkunde, 2005, 96, 1296–1300.
11. Popov V.L. Contact mechanics and friction: physical principles and applications, Springer, Berlin 2010.